PAPER

Weak-Form Discretization, Waveguide Boundary Conditions and Extraction of Quasi-Localized Waves Causing Fano Resonance

Hatsuhiro KATO[†a)], *Member and* **Hatsuyoshi KATO**[††], *Nonmember*

SUMMARY   Recently, we proposed a weak-form discretization scheme to derive second-order difference equations from the governing equation of the scattering problem. In this paper, under the scope of the proposed scheme, numerical expressions for the waveguide boundary conditions are derived as perfectly absorbing conditions for input and output ports. The waveguide boundary conditions play an important role in extracting the quasi-localized wave as an eigenstate with a complex eigenvalue. The wave-number dependence of the resonance curve in Fano resonance is reproduced by using a semi-analytic model that is developed on the basis of the phase change relevant to the S-matrix. The reproduction confirms that the eigenstate with a complex eigenvalue does cause the observed Fano resonance.

key words: Discretization, Weak form, Scattering, Waveguide boundary condition, Fano resonance

1.   Introduction

Numerov's method derives the second-order difference equation from the second-order differential equation for the scattering problem [1]. It was initially applied to one-dimensional electron conductance [2], [3] and extended to multi-dimensional problems to analyse electrode junctions [4], [5] and microwave scattering [6], [7]. The extension is performed by Fourier transformation on a lateral sub-space that is perpendicular to the direction of propagation. The same expansion of the discretization was independently developed for fibre optics by the beam propagation method [8], which is also related to Padé approximation [9], the fast Fourier transformation [10] and the finite element method [11]. Use of the Fourier transformation imposes a cyclic boundary condition on the field variable and restricts the scope of the discretization. In a previous study [7], the restriction was removed by using a weak-form discretization scheme and a Lagrangian multiplier. The weak-form theory framework provides a flexible method since it can correspond to abrupt change of the field variables by reducing the order of differential equations and also it can adopt various interpolation techniques including the Fourier series. In this study, we apply polynomial interpolation to illustrate the possibilities for using the proposed weak-form discretization scheme.

The second-order difference equation enables us to express boundary conditions of scattered waves through a stepping matrices. The concept of stepping matrices was introduced by Appelbaum [4] and redefined by Hirose and Tsukada [5] using a recursion relation [2]. In this study, the waveguide boundary condition for input and output ports is reformulated with the mode vectors of translationally invariant waveguides. The proposed condition is a type of absorbing boundary condition (ABC) [12] and is similar to the boundary condition for microwave waveguides [13]. However, it realizes perfect absorption using a numerical expression derived from the proposed discretized equation, rather than from an analytic form that is exact but not fully compatible with the numerical calculation. The origin of the numerically matching concept can be traced back to Higdon [12]. Furthermore, under the proposed weak-form discretization scheme we can extend the scope of the numerical matching to various systems which are governed by higher-order differential equations as discussed for flexural waves being governed by a fourth-order differential equation [14].

As a typical example to illustrate our scheme, we consider waves being described by the Schrödinger equation, a second-order differential equation, and analyse the Fano resonance [19] induced by the interaction between the incident wave and a quasi-localized wave in a waveguide. The significant feature of the proposed scheme is that the quasi-localized wave can be extracted as an eigenstate with a complex eigenvalue. To reproduce the resonance curve for the Fano resonance, a semi-analytic model is also developed, in which a complex eigenvalue is converted to a single pole in the wave-number space and linked to the rapid phase change of the S-matrix. The evidence for the eigenstate possessing a complex eigenvalue is confirmed by reproducing the resonance curve.

This paper is organized as follows. In Sec. 2, a Schrödinger type second order differential equation is discretized by using polynomial interpolation, then a second-order difference equation is derived as the governing equation for the scattering problem. In Sec. 3, the stepping matrix is reformulated and its application to the waveguide boundary conditions is discussed to express the behaviour of scattering waves in the input/output waveguide region. Using the waveguide boundary condition, the quasi-localized wave that causes Fano resonance is extracted as an eigenstate with a complex eigenvalue. The resonant curve is successfully reproduced by the semi-analytic model. Section 4 summarises our conclusions.
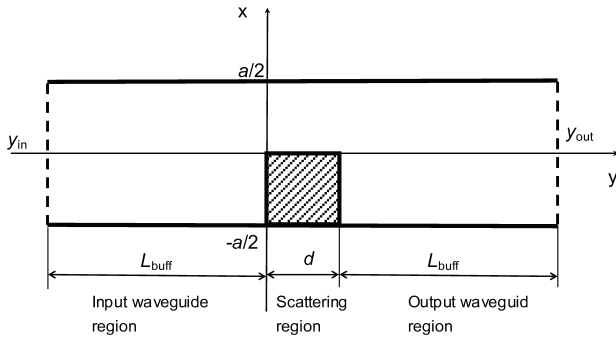
Fig. 1 System configuration. The shaded area corresponds to the potential well.

2. Weak-form discretization

2.1 Fundamental equation and system configuration

Consider a two-dimensional system in which the field variable or the wave function $u(x, y)$ is subject to the following Schrödinger-type differential equation,

$$-\nabla^2 u + \{v(x, y) - \varepsilon\}u = 0. \tag{1}$$

Here, ∇ is the nabla operator in two-dimensional space, ε is the energy or the eigenvalue and $v(x, y)$ is the potential function. The potential function is assumed to be the following well-like form,

$$v(x, y) = \begin{cases} -\varepsilon_B, & 0 \le y \le d, x < 0 \\ 0, & \text{the other region} \end{cases}, \tag{2}$$

with well depth ε_B and length d. Note that the discretization scheme proposed in this study does not depend on details of the potential function. Furthermore, our scheme is valid for any system whose governing equation can be transformed into a functional expression. Figure 1 shows the system configuration in which the linear waveguide of width a exists in the interval $y_{in} < y < y_{out}$, the scattering region is in $0 < y < d$ and the lengths of both input and output waveguides are denoted by L_{buff}. The potential function serves as a minimal model of quantum dots and lead lines in which Fano resonance has been investigated [20].

At the waveguide edges $x = \pm a/2$, the boundary condition is imposed on the field variable $u(x, y)$ as

$$u(\pm a/2, y) = 0. \tag{3}$$

The intervals $[-a/2, a/2]$ on the x-axis and $[y_{in}, y_{out}]$ on the y-axis are divided into N_x and N_y segments, respectively. Then, using the site indices ℓ (= 0, 1, 2, ..., N_x) and n (= 0, 1, 2, ..., N_y) the coordinates are discretized as follows:

$$x_\ell = x_0 + h_x \cdot \ell, \tag{4}$$
$$y_n = y_0 + h_y \cdot n. \tag{5}$$

Here, the initial values are $x_0 = -a/2$ and $y_0 = y_{in}(= -L_{buff})$,

and the step sizes are $h_x = a/N_x$ and $h_y = (y_{out} - y_{in})/N_y$.

Using the weak-form theory framework [15], the governing equation (1) can be transformed into the null value problem of a functional. A successful candidate for the functional can be derived by using Gateaux derivative [16] of the following functional $F_n[u]$,

$$F_n[u] = \frac{1}{2} \int_{S_n} \left[(\nabla u)^2 + \{v(x, y) - \varepsilon\}u^2 \right] dxdy$$

$$- \sum_{\rho=\pm} \int_{\Gamma_\rho} u(\frac{\rho a}{2}, y)\lambda_\rho dy. \tag{6}$$

Here, the integral region S_n is the narrow rectangle defined by $S_n = [-a/2, a/2] \times [y_{n-1}, y_{n+1}]$, and $\lambda_\rho(y)$ is the Lagrangian multiplier that makes the field unconstrained and imposes condition (3). The boundaries $\Gamma_\pm$ are defined by $\Gamma_\pm = \{\pm a/2\} \times [y_{n-1}, y_{n+1}]$. Unlike the typical case in the finite element method, the integral region of the functional is not the whole simulation domain but only the narrow rectangle S_n because our purpose is to derive the second-order difference equation. The functional (6) is similar but not equivalent to the expression of wave energy. The role required to the functional is to formulate the motion as a null value problem.

Using a parameter ϵ and an arbitrary field $w(x, y)$, the Gateaux derivative $F_n'[w, u]$ can be defined as follows:

$$F_n'[w, u] = \lim_{\epsilon \to 0} \frac{1}{\epsilon}\left(F_n[u + \epsilon w] - F_n[u]\right), \tag{7}$$

which is identical to the first variation of the functional [17]. The new functional $F_n'[w, u]$ can be expressed in terms of sub-functionals $F_{nS}'[w, u]$ and $F_{nL}'[w, u]$ such that

$$F_n' = F_{nS}' - F_{nL}', \tag{8}$$

$$F_{nS}' = \int_{S_n} [\nabla w \cdot \nabla u + w\{v(x, y) - \varepsilon\}u] dxdy, \tag{9}$$

$$F_{nL}' = \sum_{\rho=\pm} \int_{\Gamma_\rho} w(\frac{\rho a}{2}, y)\lambda_\rho(y)dy. \tag{10}$$

Then, the null value problem can be stated as follows: 'What is the function $u(x, y)$ that satisfies $F_n'[w, u] = 0$ for arbitrary $w(x, y)$?' The differential equation (1) with the boundary condition (3) can be derived from the null value problem [21] using the Gauss' theorem and the formula $-w\nabla^2 u = \nabla w \cdot \nabla u - \nabla(w\nabla u)$. Associated with this derivation, we can impose the constraint on $w(x, y)$ as follows:

$$w(x, y_{n\pm1}) = 0. \tag{11}$$

In deriving the differential equation from (8), this constraint removes the boundary conditions on $u(x, y)$ at $[-a/2, a/2] \times \{y_{n\pm1}\}$.

2.2 Polynomial interpolation of fields

The field $u(x, y)$ is interpolated by the values at the vertices of the lattice rectangle $S_{\ell,n} = [x_\ell, x_{\ell+1}] \times [y_{n-1}, y_{n+1}]$ as follows:

$$u(x,y) = \begin{cases} N_-(x,y)[\mathbf{u}_{\ell,n}\ \mathbf{u}_{\ell,n-1}]^T, & y_{n-1} < y < y_n \\ N_+(x,y)[\mathbf{u}_{\ell,n}\ \mathbf{u}_{\ell,n+1}]^T, & y_n < y < y_{n+1} \end{cases} \quad (12)$$

where $\mathbf{u}_{\ell,n}$ and $\mathbf{u}_{\ell,n\pm 1}$ are written in terms of field values as follows: $\mathbf{u}_{\ell,n} = [u(x_\ell, y_n)\ u(x_{\ell+1}, y_n)]^T$ and $\mathbf{u}_{\ell,n\pm 1} = [u(x_\ell, y_{n\pm 1})\ u(x_{\ell+1}, y_{n\pm 1})]^T$. The four-dimensional vector $N_\pm(x,y)$ is defined as follows:

$$N_\pm(x,y) = [1\ \ x-x_\ell\ \ y-y_n\ \ (x-x_\ell)(y-y_n)]C_\pm, \quad (13)$$

with the 4×4 matrix $C_\pm$ defined as

$$C_\pm = \begin{bmatrix} 1 & 0 & 0 & 0 \\ 1 & h_x & 0 & 0 \\ 1 & 0 & \pm h_y & 0 \\ 1 & h_x & \pm h_y & \pm h_x h_y \end{bmatrix}^{-1}. \quad (14)$$

Similarly, the arbitrary function $w(x,y)$ is expressed as

$$w(x,y) = \begin{cases} N_-(x,y)[\mathbf{w}_{\ell,n}\ \mathbf{0}]^T, & y_{n-1} < y < y_n \\ N_+(x,y)[\mathbf{w}_{\ell,n}\ \mathbf{0}]^T, & y_n < y < y_{n+1} \end{cases}, \quad (15)$$

where $\mathbf{w}_{\ell,n}$ is the four-dimensional vector defined by $\mathbf{w}_{\ell,n} = [w(x_\ell, y_n)\ w(x_{\ell+1}, y_n)]$ and the restriction that $\mathbf{w}_{\ell,n\pm 1} = \mathbf{0}$ is used to satisfy constraint (11).

Because no derivative of the potential function $v(x,y)$ is included in the functional $F'[w,u]$, the deterioration in accuracy is very small even if $v(x,y)$ is discontinuously interpolated as follows:

$$v(x,y) = \begin{cases} v_{\ell,n-\frac{1}{2}}\theta(\frac{x-x_\ell}{h_x})\theta(\frac{y-y_{n-1}}{h_y}), & y_{n-1} < y < y_n \\ v_{\ell,n+\frac{1}{2}}\theta(\frac{x-x_\ell}{h_x})\theta(\frac{y-y_n}{h_y}), & y_n < y < y_{n+1} \end{cases},$$

where $v_{\ell,n\pm\frac{1}{2}} = v(x_\ell + \frac{1}{2}h_x, y_n \pm \frac{1}{2}h_y)$ and $\theta(\xi)$ is the step-wise function defined as follows:

$$\theta(\xi) = \begin{cases} 1, & 0 < \xi < 1 \\ 0, & \xi \le 0, \xi \ge 1 \end{cases}. \quad (16)$$

2.3 Derivation of the difference equation

The integral region S_n of the functional is the union of sub-rectangles $S_{\ell,n}$ ($\ell = 0, 1, 2, ..., N_x - 1$). Therefore, the sub-functional $F'_{nS}[w,u]$ can be divided into a summation,

$$F'_{nS} = \sum_{\ell=0}^{N_x-1} \mathbf{w}_{\ell,n}^T(c_{\ell,n}\mathbf{u}_{\ell,n-1} + b_{\ell,n}\mathbf{u}_{\ell,n} + a_{\ell,n}\mathbf{u}_{\ell,n+1}). \quad (17)$$

Here, the coefficients $c_{\ell,n}$, $b_{\ell,n}$ and $a_{\ell,n}$ are 2×2 matrices defined as

$$c_{\ell,n} = c_\nabla + (v_{\ell,n-\frac{1}{2}} - \varepsilon)c_\otimes, \quad (18)$$

$$b_{\ell,n} = 2b_\nabla + (v_{\ell,n-\frac{1}{2}} + v_{\ell,n+\frac{1}{2}} - 2\varepsilon)b_\otimes, \quad (19)$$

$$a_{\ell,n} = a_\nabla + (v_{\ell,n+\frac{1}{2}} - \varepsilon)a_\otimes, \quad (20)$$

with the matrices given by

$$c_\otimes = \frac{1}{2}b_\otimes = a_\otimes = \frac{h_x h_y}{18}\begin{bmatrix} 1 & \frac{1}{2} \\ \frac{1}{2} & 1 \end{bmatrix}, \quad (21)$$

$$c_\nabla = a_\nabla = \frac{1}{6h_x h_y}\begin{bmatrix} h_y^2 - 2h_x^2 & -h_y^2 - h_x^2 \\ -h_y^2 - h_x^2 & h_y^2 - 2h_x^2 \end{bmatrix}, \quad (22)$$

$$b_\nabla = \frac{1}{6h_x h_y}\begin{bmatrix} 2(h_y^2 + h_x^2) & -2h_y^2 + h_x^2 \\ -2h_y^2 + h_x^2 & 2(h_y^2 + h_x^2) \end{bmatrix}. \quad (23)$$

The sub-functional $F'_{nL}[w,u]$ can be also expressed in the spatially discretized variables as follows:

$$F'_{nL} = \sum_{\rho=\pm} w(\frac{\rho a}{2}, y_n)\frac{h_y}{6}\{\lambda_\rho(y_{n-1}) + 4\lambda_\rho(y_{n-1})$$

$$+ \lambda_\rho(y_{n+1})\}. \quad (24)$$

Introducing the extended field vector defined by $\mathbf{U}(y_n) = [u(x_0, y_n), u(x_1, y_n), u(x_2, y_n), ..., u(x_{N_x}, y_n)]^T$, and expressing the summation in the extended matrix form, the null value problem $F'_n[w,u] = 0$ for arbitrary $w(x_\ell, y_n)$ yields the following:

$$\bar{c}_n\mathbf{U}(y_{n-1}) + \bar{b}_n\mathbf{U}(y_n) + \bar{a}_n\mathbf{U}(y_{n+1}) - E\mathbf{\Lambda}_n = 0. \quad (25)$$

Here, $\bar{c}_n$, $\bar{b}_n$ and $\bar{a}_n$ are $(N_x+1) \times (N_x+1)$ matrices whose non zero elements are composed from the 2×2 matrices. For $\bar{c}_n$, $\bar{c}_n(\ell, \ell) = (1 - \delta_{\ell,N_x})c_{\ell,n}(1,1) + (1 - \delta_{\ell,0})c_{\ell-1,n}(2,2)$, $\bar{c}_n(\ell, \ell+1) = c_{\ell,n}(1,2)$ and $\bar{c}_n(\ell, \ell-1) = c_{\ell-1,n}(2,1)$. The matrices $\bar{b}_n$ and $\bar{a}_n$ are also defined by the same rule. Hereafter the matrix with super bar, $\bar{\ }$, is of size $(N_x + 1) \times (N_x + 1)$. The $(N_x + 1) \times 2$ matrix E is defined as follows:

$$E = \begin{bmatrix} 1 & 0 & 0 & \cdots & 0 & 0 \\ 0 & 0 & 0 & \cdots & 0 & 1 \end{bmatrix}^T, \quad (26)$$

and the Lagrangian multipliers are summarized in the two-dimensional vector as follows:

$$\mathbf{\Lambda}_n = \frac{h_y}{6}\begin{bmatrix} \lambda_-(y_{n-1}) + 4\lambda_-(y_n) + \lambda_-(y_{n+1}) \\ \lambda_+(y_{n-1}) + 4\lambda_+(y_n) + \lambda_+(y_{n+1}) \end{bmatrix}. \quad (27)$$

Multiplying the term $E^T\bar{b}_n^{-1}$ from the left to both sides of (25) and using the boundary condition (3), or equivalently $E^T\mathbf{U}(y_n) = 0$, we obtain the following relation:

$$E\mathbf{\Lambda}_n = E\{E^T(\bar{b}_n^{-1}\bar{E})\}^{-1}\bar{c}_n\mathbf{U}(y_{n-1})$$

$$+ E\{E^T(\bar{b}_n^{-1}\bar{E})\}^{-1}\bar{a}_n\mathbf{U}(y_{n+1}). \quad (28)$$

Substituting (28) for the term $E\mathbf{\Lambda}_n$ in the difference equation (25) yields

$$\bar{c}'_n\mathbf{U}(y_{n-1}) + \bar{b}_n\mathbf{U}(y_n) + \bar{a}'_n\mathbf{U}(y_{n+1}) = 0, \quad (29)$$

where

$$\bar{c}'_n = \bar{c}_n - E\{E^T(\bar{b}_n^{-1}E)\}^{-1}\bar{c}_n, \quad (30)$$

$$\bar{a}'_n = \bar{a}_n - E\{E^T(\bar{a}_n^{-1}E)\}^{-1}\bar{a}_n. \quad (31)$$

Thus, we have transformed the partial differential equation (1) into the second-order difference equation (29). A remarkable feature of difference equation appears in coefficients $\bar{c}'_n$ and $\bar{a}'_n$ in which the boundary condition at $x = \pm a/2$ is already captured by the modulation terms. This feature is obtained by using compatibility of the weak-form theory framework with Lagrangian multipliers.

3. Quasi-localized waves in Fano resonance

3.1 Waveguide boundary condition

The waveguide regions in Fig. 1 serve as the input and output ports of the scattering region. Because the system is in a steady state and no scatterer exits in the input and output waveguides, the wave in the waveguide can be expressed by the superposition of the waveguide modes $e^{\eta_p y} X_p(x)$ where $X_p(x)$ is the mode function, η_p is the wave constant and $p(= 1, 2, 3, ..., N_x + 1)$ is the mode index. The real and imaginary parts of η_p are the growing/dampening rate of wave amplitude and the wave number along the y-axis, respectively. Let us introduce the mode vector as $\mathbf{X}_p = [X_p(x_0) \, X_p(x_1) \, ... X_p(x_{N_x})]^T$, then $\mathbf{X}_p$ and η_p are found through the eigenvalue problem, which will be defined by (34) below. Let us also introduce the reciprocal vector $\tilde{\mathbf{X}}_p$ which satisfies the relation $\tilde{\mathbf{X}}_p^\dagger \mathbf{X}_q = \delta_{pq}$, where $\dagger$ denotes the Helmite conjugate and δ_{pq} is the Kronecker delta.

The stepping matrix $\bar{K}_{wg}$ originally introduced by Appelbaum [4] can be redefined as follows:

$$\bar{K}_{wg} = \sum_p e^{\eta_p h_y} \mathbf{X}_p \tilde{\mathbf{X}}_p^\dagger. \tag{32}$$

Because of the relation $\left(\bar{K}_{wg}\right)^n = \sum_p e^{\eta_p h_y n} \mathbf{X}_p \tilde{\mathbf{X}}_p^\dagger$, the n-dependence of the field vector $\mathbf{U}(y_n)$ can be expressed as follows:

$$\mathbf{U}(y_n) = \left(\bar{K}_{wg}\right)^{(n-n_0)} \mathbf{U}(y_{n_0}), \tag{33}$$

where n_0 is an appropriate site index in the input/output waveguide region. The purpose of the matrix $\bar{K}_{wg}$ is to advance the field vector $\mathbf{U}(y_n)$ by one step along the y-axis; this gives rise to the terminology of a *stepping matrix*.

The input/output waveguide is translationally invariant, namely, the property of the waveguide is uniform and does not depend on the y-axis. Therefore, the coefficient matrices $\bar{c}'_n$, $\bar{b}_n$ and $\bar{a}'_n$ in (29) are independent of the index n, and the n-dependence of the coefficients degenerates. The matrices can be expressed as constant matrices $\bar{a}'_{wg}$ and $\bar{b}_{wg}$ with $\bar{c}'_n = \bar{a}'_n = \bar{a}'_{wg}$ and $\bar{b}_n = \bar{b}_{wg}$. We find that the mode vector $\mathbf{X}_p$ satisfies the following relation,

$$-\bar{b}_{wg} \mathbf{X}_p = 2\cosh(\eta_p h_y) \bar{a}'_{wg} \mathbf{X}_p. \tag{34}$$

This equation is a kind of generalized eigenvalue problem [22]; therefore, the eigenvector $\mathbf{X}_p$ and the eigenvalue $2\cosh(\eta_p h_y)$ can be accurately obtained by using the well-defined numerical procedure [23].

Because the function cosh is even, the values of η_p and $-\eta_p$ are both the wave constants with the same eigenvector $\mathbf{X}_p$. If the wave constant η_p is real (purely imaginary), the waveguide mode acts as a growing/dampening wave (travelling wave). The growing/dampening property of the mode amplitude along the y-axis is consistent with the continuum system being subject to (1). This consistency

is a very useful feature what allows us to use solutions from the discretized system subjected to the second-order difference equation (29) to approximate waves in the continuum system.

Because the system is also invariant under time-inversion, if η_p is a wave constant, not only the inverted value $-\eta_p$ but also its complex conjugate η_p^* is the wave constant. Using space- and time-reversal symmetries, we can choose the $N_x + 1$ wave constants so as to satisfy $\text{Im}[\eta_p] > 0$ and $\text{Re}[\eta_p] < 0$. Then, the stepping matrix $\bar{K}_{wg}$ is denoted by $\bar{K}_+^{(dmp)}$. The application of $\bar{K}_+^{(dmp)}$ to the field vector $\mathbf{U}(y_n)$ is divided into the following three steps: (i) Decompose the wave into the superposition of waveguide modes, (ii) increase the phases of the travelling waveguide modes of the pure imaginary η_p by an amount $\text{Im}[\eta_p h_y]$, and (iii) dampen the wave amplitudes of the non-travelling waveguide modes by the factor $e^{-|\text{Re}[\eta_p]| h_y}$.

When the input/output waveguide is uniform and no potential exits, *i.e.* $v(x, y) = 0$, the wave constant η_q is either real or purely imaginary and is expressed as $\eta_q = [(\pi q/a)^2 - \varepsilon]^{1/2}$ ($q = 1, 2, 3, ...$). The mode denoted by the index q is a travelling wave, if and only if the parameter ε is larger than the cut-off energy $\varepsilon_q^{(cut)} = (\pi q/a)^2$.

3.2 Eigenvalue problem defined by waveguide boundary conditions

3.2.1 Resonance curve

Let us consider the scattering problem when the incident wave comes from the input end $y = -L_{buff}$. If the energy of the incident wave, ε, is in the interval between the first and second cut-off energies, $\varepsilon_1^{(cut)} < \varepsilon < \varepsilon_2^{(cut)}$, the reflection and transmission waves appearing in the input and output waveguide regions take the same travelling mode of $\mathbf{X}_1$. Figure 2 shows the k-dependence of the reflection rate $|r(k)|^2$ which is numerically calculated by the recursive transfer method (RTM). Details about RTM are given in Ref. [7], but the resulting expression for the transmission coefficient $r(k)$ is introduced in (41) below. Here, k is the wave-number along the y-axis and it is dimensionlessly defined by

$$k = \{\varepsilon - \varepsilon_1^{(cut)}\}^{1/2}. \tag{35}$$

The geometry of the system are also dimensionlessly expressed and assumed to be as follows: the scattering length $d = 1$, the potential depth $\varepsilon_B = 80$, the waveguide width $a = 0.8$, and the length of the input and output waveguides $L_{buff} = 2.5$. The numbers of divisions of the coordinates are $N_x = 40$ and $N_y = 300$, which means that the both step sizes are the same $h_x = h_y = 0.02$.

We have shown that the discrepancies between wave strengths of analytical and RTM expressions are less than the order of h_y^4 when a plane wave propagates along the y-axis [7]. We have also compared the transmission rates obtained by RTM with what obtained by the finite element method [7] and an experiment [18] about a microwave scattering problem. Although these comparisons are concerned
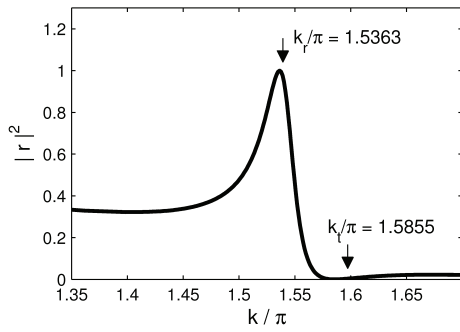
Fig. 2 Resonance curve for the reflection rate $|r|^2$ under Fano resonance. The arrows show the wave number for full reflection, k_r, and full transmission, k_t.

with the microwave, these convinces us the accuracy of the results obtained by RTM being formulated under the weak-form discretization scheme because the governing equations of both systems are the same kind of second-order differential equations.

The k-dependence of the reflection rate $|r(k)|^2$ reaches its maximum at $k_r = 1.5363\pi$ (that is, $|r(k_r)|^2 = 1$), as shown in Fig. 2. The resonance curve has the asymmetry that is type of Fano resonance [19]. At $k_t = 1.5855\pi$, the reflection rate $|r(k)|^2$ vanishes and full transmission is realized. The wave-numbers k_r and k_t are transformed by (35) into the energies $\epsilon_r = 38.7153$ and $\varepsilon_t = 40.2335$, respectively. Fano resonance is caused by interactions between the incident wave and any localized or quasi-localized wave formed around the scatterer. The localized waves can be found as an eigenstate defined by our proposed difference equation and waveguide boundary conditions, as shown in the next section.

3.2.2 Quasi-localized wave as an eigenstate

When the wave amplitude has a local peak in the scattering region, the skirts or tails of the peak penetrate into the output and input waveguide regions. In the output waveguide region, the amplitude of the penetrated wave is dampened along the positive direction of the y-axis. Therefore, the dampening behaviour of the wave can be expressed by the stepping matrix $\bar{K}_+^{(dmp)}$. If any travelling wave is generated by the local peak, it travels in the positive direction to the output waveguide region; the positive sign of the subscript in $\bar{K}_+^{(dmp)}$ reflects this situation. On the opposite side in the input waveguide region, the amplitude grows along the positive direction but the travelling direction of the wave skirt may take either direction. For a strict localized wave, the choice of the double sign $\pm$ in the subscript on $\bar{K}_\pm^{(grw)}$ is not important because it has no travelling wave skirts but it does have growing amplitudes along the positive direction of the y-axis, which are the dampening outgoing tails. However, for a quasi-localized wave with travelling skirts, the choice of the double sign defines the travelling direction of the wave skirt either the skirt is an outgoing wave or it is

connected to the stimulating input wave.

If a quasi-localized wave has outgoing wave skirts, the boundary condition at the waveguides is expressed as follows:

$$\mathbf{U}(y_{-1}) = \left(\bar{K}_-^{(grw)}\right)^{-1}\mathbf{U}(y_0), \quad \mathbf{U}(y_{N_y+1}) = \bar{K}_+^{(dmp)}\mathbf{U}(y_{N_y}).$$
(36)

Furthermore, if an incident wave coherently couples with a quasi-localized wave without the reflection wave, the waveguide boundary condition changes to the following:

$$\mathbf{U}(y_{-1}) = \left(\bar{K}_+^{(grw)}\right)^{-1}\mathbf{U}(y_0), \quad \mathbf{U}(y_{N_y+1}) = \bar{K}_+^{(dmp)}\mathbf{U}(y_{N_y}),$$
(37)

where the sign of the subscript on the stepping matrix in the first expression differs from that in the former condition. In this case, the reflection rate vanishes and a full transmission is realized.

The quasi-localized wave that causes Fano resonance can be obtained by solving (29) as an eigenvalue problem for the eigenvalue ε. Because the fundamental equation (1) is linear in the parameter ε, we can separate the coefficients in (29) into two parts according to whether they are proportional to ε: $\bar{c}_n' = \bar{c}_n^{(1)} - \varepsilon\bar{c}_n^{(2)}$, $\bar{b}_n = \bar{b}_n^{(1)} - \varepsilon\bar{b}_n^{(2)}$ and $\bar{a}_n' = \bar{a}_n^{(1)} - \varepsilon\bar{a}_n^{(2)}$. Then, (29) can be expressed as follows:

$$\bar{c}_n^{(1)}\mathbf{U}(y_{n-1}) + \bar{b}_n^{(1)}\mathbf{U}(y_n) + \bar{a}_n^{(1)}\mathbf{U}(y_{n+1})$$
$$= \varepsilon\left\{\bar{c}_n^{(2)}\mathbf{U}(y_{n-1}) + \bar{b}_n^{(2)}\mathbf{U}(y_n) + \bar{a}_n^{(2)}\mathbf{U}(y_{n+1})\right\},$$
(38)

for $0 \le n \le N_y$. If a new $(N_x+1)(N_y+1)$-dimensional vector $\mathbf{U}_{tot}$ is introduced as $\mathbf{U}_{tot} = [\,\mathbf{U}(y_0)\,\mathbf{U}(y_1)\,\mathbf{U}(y_2)\,...\,\mathbf{U}(y_{N_y})]^T$, then (38) serves as an eigenvalue problem with eigenvalue ε. Using the boundary condition (37), we can eliminate the vectors $\mathbf{U}(y_{-1})$ and $\mathbf{U}(y_{N_y+1})$ that appear when $n = 0$ and N_y, respectively. Note that this eigenvalue problem is valid even if any dampening wave tails and/or travelling wave skirts reach ends of the simulation domain. This property is an advantage to analyse the scattering problem with localized waves through the proposed scheme.

The eigenvalue ε can be found from the eigenvalue problem (38) provided that the stepping matrices $K_\pm^{(grw)}$ and $K_+^{(dmp)}$ are already defined with a preliminary value of ε. The consistency between the preliminary ε and the eigenvalue ε is realized through iterative use of the eigenvalue ε for defining the stepping matrices in the successively repeated eigenvalue problems.

Figure 3 (a) shows the resulting wave form of the quasi-localized wave with the boundary condition (36). The eigenvalue is the complex number $\varepsilon_L = 38.898 - 0.465968i$, where the imaginary part reflects the finite life time caused by the outgoing wave skirts. The converted wave-number has the value $k_L = (1.5425 - 0.0153i)\pi$ and it is very similar to k_r for full reflection rather than k_t for full transmission. Figure 3 (b) shows the quasi-localized wave with boundary condition (37). The eigenvalue is $\varepsilon_T = 40.2335$ and the converted wave-number is $k_T = 1.5855\pi$, which is strictly
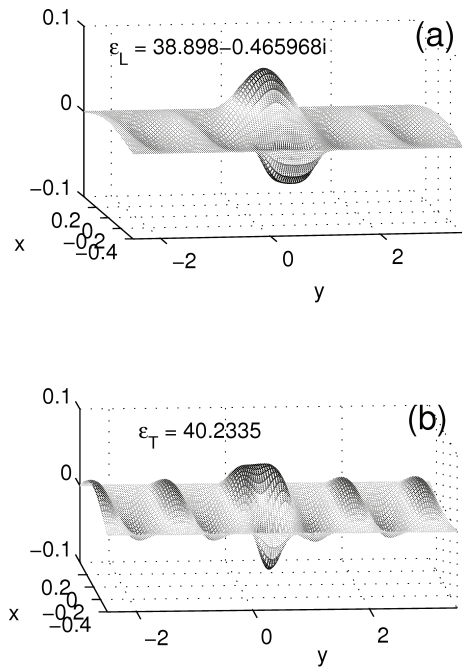
Fig. 3 Wave forms of the eigenstate. (a) Quasi-localized wave that possesses the complex eigenvalue ε_L and emits outgoing wave skirts. (b) Full transmission wave with the real eigenvalue ε_T and wave skirts which are coherently coupled to the incident wave.

Fig. 4 Resonance curve and the semi-analytic model. (a) The k-dependence of $\sin^2\delta$ is obtained by RTM (solid curve) and the reproduced curve by the semi-analytic model (dashed curve). (b) Sub-phases δ_+ and δ_- are obtained from RTM. (c) Total phase $\delta(=\delta_+ + \delta_-)$ and background phase δ_{bg}.

equivalent to k_t.

The shape of the quasi-localized wave in the scattering region is similar to the second-order waveguide mode which can penetrate but not travel beyond the scattering region because of the assumption $\varepsilon_1^{(cut)} < \varepsilon < \varepsilon_2^{(cut)}$.

3.3 Semi-analytic model of the resonance

According to the scattering theory for one-dimensional system [24], the resonance curve is related to the single pole of the reflection and transmission coefficients as an analytic function in wave-number space. Furthermore, the single pole is linked to either localized or quasi-localized wave. The system in this study can be regarded as quasi one-dimensional if the wave energy ε is between the first and second cut off energies. In this section, we show that the resonance curve can be reproduced by using the complex wave number k_L.

According to the formulation of RTM, the field vectors of the reflection wave, $\mathbf{U}_{rf}$, and the transmission wave, $\mathbf{U}_{tr}$, are expressed as follows:

$$\mathbf{U}_{rf} = -(S_0 - K_-^{(grw)})^{-1}(S_0 - K_+^{(dmp)}), \tag{39}$$

$$\mathbf{U}_{tr} = S_{N_y-1} \cdots S_2 S_1 S_0 (\mathbf{U}_{in} + \mathbf{U}_{rf}), \tag{40}$$

where $S_n(k)$ is the stepping matrix at the n-th site [7]. Because of the assumption on the wave energy, only one travelling mode exits in the waveguide region. The travelling
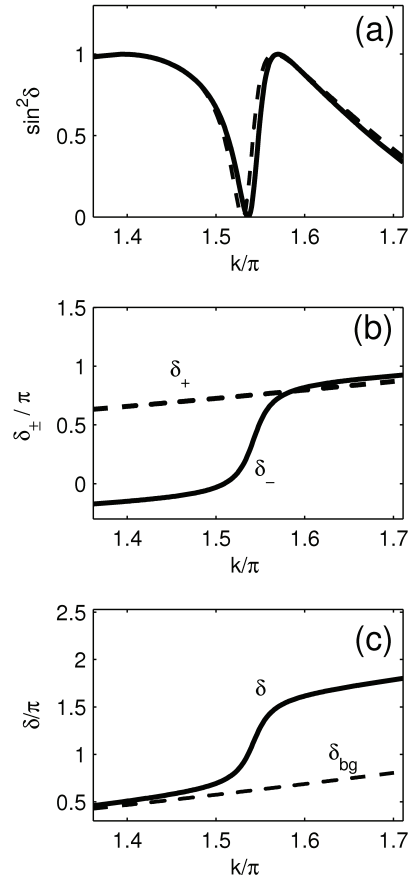
mode vector and its reciprocal vector were denoted as $\mathbf{X}_1$ and $\tilde{\mathbf{X}}_1$, respectively. Therefore, the reflection and transmission coefficients $r(k)$ and $t(k)$, are expressed as follows:

$$r = \tilde{\mathbf{X}}_1^\dagger \mathbf{U}_{rf}, \quad t = \tilde{\mathbf{X}}_1^\dagger \mathbf{U}_{tr}. \tag{41}$$

Because the system is symmetric under y-axis and time inversions, we can obtain the following relations: $|r(k)|^2 + |t(k)|^2 = 1$ and $r(k)^* t(k) + r(k)t^*(k) = 0$. These relations are also numerically confirmed with errors smaller than 5×10^{-15}.

The S-matrix combines inputs and outputs which are coming and going waves from both ends of the simulation domain. Using the reflection and transmission coefficients, $r(k)$ and $t(k)$, the S-matrix $S(k)$ can be expressed as follows:

$$S(k) = \begin{bmatrix} r(k) & t(k) \\ t(k) & r(k) \end{bmatrix}, \tag{42}$$

and the determinant is given by $\det S(k) = \{r(k)+t(k)\}\{r(k)-$

$t(k)$}. Conservation of energy requires $S(k)^\dagger S(k) = I_2$ with the 2×2 unit matrix I_2. Therefore, the determinant $\det S(k)$ and its factors $r(k) \pm t(k)$ are unitary and can be expressed as $\det S(k) = e^{i2\delta(k)}$ and $r(k) \pm t(k) = e^{i2\delta_\pm(k)}$ with real phases $\delta(k)$ and $\delta_\pm(k)$.

Using the analogy of scattering theory in three-dimensional space [25], a quantity similar to the cross section can be defined by $\sin^2 \delta(k)$, whose k-dependence has the resonant behaviour shown in Fig. 4 (a). In Fig. 4 (b) and 4 (c), the k-dependences of the phases $\delta_\pm(k)$ and $\delta(k)$ are shown in which the rapid phase change corresponds to the resonant behaviour in Fig. 4 (a). Furthermore, the rapid phase change of $\delta(k)$ is because of the sub-phase $\delta_-(k)$. It should be also pointed out that a rapid phase change of $\delta(k)$ caused by another sub-phase $\delta_+(k)$ is possible under different situations.

Assuming that the single pole at k_L in k-space causes the rapid phase change, the determinant $\det S(k)$ in the neighbourhood of k_L can be approximately expressed as follows [25]:

$$\det S(k) \approx e^{i2\delta_{\text{bg}}(k)} \frac{k - k_L^*}{k - k_L}. \tag{43}$$

This expression satisfies the following two necessary conditions: (i) $|\det S(k)|^2 = 1$ and (ii) the pole is of order one. The background phase $\delta_{\text{bg}}(k)$ corresponds to the slow change when the resonant is absent and its k-dependence is estimated by the broken curve shown in Fig. 4 (b). The broken curve is the extrapolation of a quadratic curve that approximates the solid curve in the region $k < 1.0 \cdot \pi$ where the influence of the resonance is minor. Regarding the phase of (43) as $\delta(k) \approx \delta_{\text{bg}}(k) + \delta_{\text{res}}(k)$ with the resonance phase $\delta_{\text{res}}(k)$ and using the quantities defined by $q(k) = \cot \delta_{\text{bg}}(k)$ and $\epsilon(k) = (k - \text{Re}[k_L])/\text{Im}[k_L]$, we can find

$$\sin^2 \delta(k) \approx \frac{(q + \epsilon)^2}{(1 + q^2)(1 + \epsilon^2)}, \tag{44}$$

where the relation $\tan 2\delta_{\text{res}}(k) = (1 - \epsilon^2)/2\epsilon$ was used [26].

The result (44) is a semi-analytic expression that was derived by considering the analytic feature of the S-matrix. Although the denominator has the extra factor $(1 + q^2)$ compared to Fano's original equation [19], the asymmetry caused by the parameter $q(k)$ is still maintained, as has already been pointed out [26]. The resonance curve given by (44) is shown as the broken curve in Fig. 4 (a), which falls close to the solid curve. Both curves fall to zero at the wavenumbers 1.536π (solid curve) and 1.531π (broken curve) and the discrepancy is less than 0.4 %. The agreement of these two curves convinces us that the quasi-localized wave of the complex eigenvalue, which might be considered as an artificial construct, does cause the resonance of the experimentally observable quantity.

4. Conclusions

Using flexibility that the weak-form discretization scheme can adopt various interpolation techniques, a Schrödinger type second-order differential equation was transformed into a second-order difference equation by polynomial interpolation. The behaviour of the solutions derived from the second-order difference equation is consistent with that of waves in the original continuum system with respect to amplitude variations due to both travelling and growing/dampening waves. This consistency enables us to approximate scattering waves in the continuum system by the discretized system and to define the waveguide boundary conditions numerically as perfectly ABC. This is an advantage to use the second-order difference equation.

Using the waveguide boundary condition, we also proposed a new method for extracting the quasi-localized wave as an eigenstate by iteratively solving an eigenvalue problem. The validity of our scheme was confirmed by investigating Fano resonance with a semi-analytic model in which the quasi-localized wave possessing the complex eigenvalue corresponds to a single pole in wave-number space. According to our knowledge, this study is the first one to propose a strictly defined numerical procedure to regard the localized/quasi-localized wave as an eigenstate.

References

[1] F. Y. Hajj, H. Kobeisse and N. R. Nassif, "On the numerical solution of shroedinger's radial equation", Journal of Computational Physics, vol.16, pp.150-159, 1974.

[2] Ph. Lambin and J. P. Vigneron, "Improved continued fraction treatment of the one-dimensional scattering problem", J. Phys. A (Math. Gen.), vol. 14, pp. 1815-1819, 1981.

[3] J. P. Vigneron and Ph. Lambin "Improved continued fraction treatment of the one-dimensional scattering problem", Journal of Physics A (Math. Gen.), vol. 13, p.1135, 1980.

[4] J. A. Appelbaum and D. R. Hamann, "Self-consistent electronic structure of solid surfaces", Physical Review B, vol.6, pp.2166-2177, 1972.

[5] K. Hirose and M. Tsukada, "First-principles calculation of the electronic structure for a bielectrode junction system under strong field and current", Physical Review B vol.51, no.8, pp.5278-5290, 1995.

[6] H. Kato and Y. Kanno, "Microwave absorption of catalyst in a thermal decomposition reaction by recursive transfer method", Japanese Journal of Applied Physics, vol.47, no.6, pp.4846-4850, 2008.

[7] H. Kato and H. Kato, "New formulation for the recursive transfer method using the weak form thery framework and its application to microwave scattering", Transactions of IEICE-A, vol.E96-A,no.12, pp. 2698-2708, 2013.

[8] M. D. Feit and J. A. Fleck, "Light propagation in graded-index optical fibers", Applied optics, vol. 17, no. 34, pp. 3990-3998, Dec. 1978.

[9] G. R. Hadley, "Wide-angle beam propagation using Padé approximatimant optics", Optical letters, vol. 17 no. 20, pp. 1426-1468,1992.

[10] M. D. Feit andJ . A. Fleck, "Light propagation in graded-index optical fibers", Applied optics, vol. 17, no. 34, pp. 3990-3998,1978.

[11] M Koshiba and Y. Tsuji, "A wide-angle finite-element beam propagation method", IEEE photonics technology letters, vol. 8, no. 9, pp. 1208-1210, 1996. IEEE phot. tech. lett. 8 (1996), 1208-1210.

[12] R L. Higdon, "Absorbind boundary conditon for difference appeximation to the multi-dimensional wave equation", Mathematics of

Computation vol. 47, no. 176, pp. 437-459, 1986.

[13] Z. Lou and J. M. Jin, "An accurate waveguide port boundary condition for the time-domain finite-element method", IEEE Trans. Microwave Ther. & Tech., vol. 53, no. 9, pp. 3014-3023, 2005.

[14] H. Kato and H. Kato, "Application of the recursive transfer method to flexural waves I: Novel discretization scheme using weak form theory framework and waveguide modes on inhomogeneous elastic plates", Transactions of IEICE-A, vol. E97-A, no. 5, 2014 (in printing).

[15] M. J. Forray, Variational calculus in science and engineering, McGraw Hill, New York, 1968.

[16] Per Heintz and Klas Samuelsson, "On adaptive strategies and error control in fracture mechanics", Computers and Structures, pp. 485-497 vol. 82, Iss. 6, 2004.

[17] K. Rektorys, Variational methods in mathematics, science and engineering, D. Reidel Pub., Dordrecht, 1975.

[18] H. Kato, M. Kitani and H. Kato, "Proposal of Recursive Transfer Method as an Accurate Numerical Method for Microwave Scattering Problem", Asia-Pasific Readio Science Conference 2010, prg. no. BEFKc-2, Toyama Japnan, Sep. 22-26 2010.

[19] U. Fano, "Effects of configuration interaction on intensities and phaseshifts", Physical Revies vol. 124, pp. 1866-1878, 1961.

[20] A. E. Miroshnichenko, "Fano resonances in nanoscale structures", Reviews of Modern Physics, vol. 82, no. 3, pp.2257-2298, 2010.

[21] P. Solín , Partial differential equations and the finite element method, John Wiley & Sons, Hoboken 2006.

[22] K. J. Bathe and E. L. Wilson, Numerical methods in finite element analysis, Prentice-Hall, New York 1976.

[23] L. Ramdas Ram-Mohan, Finite Element and Boundary Element Applications in Quantum Mechanics, p. 373, Oxford Unv. Press, Oxford 2002.

[24] G. L. Lamb, Elements of soliton theory, John Wiley & Sons, New Yourk, 1985.

[25] John, R. Taylor, Scattering Theory, John Wiley & Sons, New York 1972.

[26] K. Shimamura, "Fundamentals of resonance scattering physics", Journal of Atomic Collision Research (Japanese Edition), vol. 2, no. 2, pp. 6-19, 2005.